THE JOURNAL OF BIOLOGICAL CHEMISTRY VOL. 284, NO. 51, pp. 35495–35506, December 18, 2009

Direct Sensing of Intracellular pH by the Cystic Fibrosis Transmembrane Conductance Regulator (CFTR) Cl^- Channel*[S]◆

Received for publication, October 5, 2009 Published, JBC Papers in Press, October 16, 2009, DOI 10.1074/jbc.M109.072678

Jeng-Haur Chen[1], **Zhiwei Cai, and David N. Sheppard**[2]

From the Department of Physiology and Pharmacology, University of Bristol, School of Medical Sciences, University Walk, Bristol BS8 1TD, United Kingdom

In cystic fibrosis (CF), dysfunction of the cystic fibrosis transmembrane conductance regulator (CFTR) Cl^- channel disrupts epithelial ion transport and perturbs the regulation of intracellular pH (pH_i). CFTR modulates pH_i through its role as an ion channel and by regulating transport proteins. However, it is unknown how CFTR senses pH_i. Here, we investigate the direct effects of pH_i on recombinant CFTR using excised membrane patches. By altering channel gating, acidic pH_i increased the open probability (P_o) of wild-type CFTR, whereas alkaline pH_i decreased P_o and inhibited Cl^- flow through the channel. Acidic pH_i potentiated the MgATP dependence of wild-type CFTR by increasing MgATP affinity and enhancing channel activity, whereas alkaline pH_i inhibited the MgATP dependence of wild-type CFTR by decreasing channel activity. Because these data suggest that pH_i modulates the interaction of MgATP with the nucleotide-binding domains (NBDs) of CFTR, we examined the pH_i dependence of site-directed mutations in the two ATP-binding sites of CFTR that are located at the NBD1:NBD2 dimer interface (site 1: K464A-, D572N-, and G1349D-CFTR; site 2: G551D-, K1250M-, and D1370N-CFTR). Site 2 mutants, but not site 1 mutants, perturbed both potentiation by acidic pH_i and inhibition by alkaline pH_i, suggesting that site 2 is a critical determinant of the pH_i sensitivity of CFTR. The effects of pH_i also suggest that site 2 might employ substrate-assisted catalysis to ensure that ATP hydrolysis follows NBD dimerization. We conclude that the CFTR Cl^- channel senses directly pH_i. The direct regulation of CFTR by pH_i has important implications for the regulation of epithelial ion transport.

The ATP-binding cassette (ABC)[3] transporter cystic fibrosis transmembrane conductance regulator (CFTR) (1) is a multifunctional protein best known as a regulated Cl^- channel (2). CFTR is assembled from five domains: two membrane-spanning domains (MSDs) that form an anion-selective pore, two nucleotide-binding domains (NBDs) that bind and hydrolyze ATP to control channel gating, and a unique regulatory domain (RD), whose phosphorylation by PKA is critical for CFTR activation (2, 3). CFTR is principally expressed in the apical membrane of epithelia throughout the body where it plays a fundamental role in fluid and electrolyte movements (4). Malfunction of CFTR causes the common genetic disease cystic fibrosis (CF) (4).

Previous studies demonstrate that the regulation of intracellular pH (pH_i) is defective in CF epithelial cells (*e.g.* Ref. 5). They also reveal that expression of recombinant CFTR in heterologous cells modulates pH_i (*e.g.* Ref. 6). Analysis of the literature suggests that CFTR modulates pH_i in three main ways. First, CFTR itself directly transports HCO_3^- ions with a modest permeability ($P_{HCO_3^-}/P_{Cl^-}$ ~0.26 (7)). Second, CFTR regulates the Na^+/H^+ exchanger isoform 3 (NHE3), which contributes to Na^+-dependent HCO_3^- reabsorption in pancreatic duct epithelia. CFTR stabilizes NHE3 expression at the cell surface and inhibits NHE3 activity by a cAMP-dependent mechanism when pancreatic HCO_3^- secretion is stimulated (8). Of note, the regulation of NHE3 by CFTR involves the association of CFTR and NHE3 with the scaffolding protein EBP50 to form a macromolecular complex (8). Third, CFTR regulates the Cl^-/HCO_3^- (anion) exchanger (AE), which plays a central role in pancreatic HCO_3^- secretion. CFTR regulation of AE requires the cell surface expression and cAMP-dependent phosphorylation of CFTR, but not its transport of anions (6). Interestingly, Ko *et al.* (9) demonstrated that CFTR and members of the SLC26 family of AEs coordinate their activities through the interaction of the, phosphorylated RD of CFTR with the STAS (sulfate transporter and antisigma-factor antagonist) domain of SLC26 transporters. Thus, CFTR modulates pH_i through its roles as an ion channel and regulator of transport proteins.

A key unresolved question is how CFTR senses changes in pH_i. As described above, CFTR might detect pH_i changes indirectly through its interactions with NHE3 and SLC26 transporters. Consistent with this idea, Reddy *et al.* (10) demonstrated that pH_i modulates indirectly the CFTR Cl^- conductance of sweat duct epithelia by altering the enzymatic

* This work was supported by the Cystic Fibrosis Trust.
◆ This article was selected as a Paper of the Week.
[S] The on-line version of this article (available at http://www.jbc.org) contains supplemental "Experimental Procedures," "Results," Equations 2 and 3, references, Tables 1–5, and Figs. 1–4.
[1] Supported by the University of Bristol and an Overseas Research Student award. Current address and to whom correspondence may be addressed: Howard Hughes Medical Institute, Dept. of Internal Medicine, Roy J. and Lucille A. Carver College of Medicine, University of Iowa, 500 EMRB, Iowa City, IA 52242. Tel.: 319-335-6540; Fax: 319-335-7623; E-mail: jeng-haur-chen@uiowa.edu.
[2] To whom correspondence may be addressed. Tel.: 44-117-331-2290; Fax: 44-117-331-2288; E-mail: D.N.Sheppard@bristol.ac.uk.
[3] The abbreviations used are: ABC, ATP-binding cassette; AE, Cl^-/HCO_3^- (anion) exchanger; Bis-Tris, 2-[Bis(2-hydroxyethyl)imino]-2-(hydroxymethyl)-1,3-propanediol; CF, cystic fibrosis; CFTR, cystic fibrosis transmembrane conductance regulator; *i*, single-channel current amplitude; IBI, interburst interval; MBD, mean burst duration; *N*, number of active channels; NBD, nucleotide-binding domain; NHE3, Na^+/H^+ exchanger isoform 3; PKA, protein kinase A; P_o, open probability; RD, regulatory domain; SAC, substrate-assisted catalysis; TAP, transporter associated with antigen processing; TES, *N*-tris[hydroxymethyl]methyl-2-aminoethanesulfonic acid; Tris, tris(hydroxymethyl)aminomethane.

activities of the protein kinases and phosphatases that control the phosphorylation status of CFTR. However, the ATPase activity of some ABC transporters (*e.g.* the transporter associated with antigen processing (TAP)) is pH_i-dependent (11), while the ATPase activity of an NBD1-RD-CFTR fusion protein is optimal at neutral pH (12). These data raise the possibility that pH_i might regulate directly CFTR activity. To test this hypothesis, we used excised inside-out membrane patches from cells expressing recombinant wild-type human CFTR. When we observed that pH_i has multiple effects on the single-channel activity of CFTR, we used CFTR constructs containing site-directed mutations to explore the molecular mechanisms of CFTR regulation by pH_i.

EXPERIMENTAL PROCEDURES

Cells and CFTR Expression—In this study we used mammalian cells heterologously expressing CFTR constructs. Where available, we used cells stably expressing CFTR constructs. These included (i) mouse mammary epithelial cells (C127 cells) expressing wild-type human CFTR, the CFTR variant ΔR-S660A (13) or the CF mutant G1349D (14), (ii) Fischer rat thyroid epithelial cells expressing the CF mutant G551D (15), and (iii) NIH-3T3 cells expressing the CFTR construct K1250M (16). To study the CFTR variants K464A, D572N, and D1370N, we employed the vaccinia virus/bacteriophage T7 hybrid expression system to transiently express CFTR variants in HeLa cells as described previously (17, 18). As a control, we verified that the single-channel behavior of wild-type human CFTR in different mammalian cells was equivalent (for further information, see supplemental "Results" and Figs. 1 and 2).

HeLa cells were purchased from the American Type Culture Collection (Manassas, VA). C127 cells expressing wild-type CFTR were a generous gift of Dr. C. R. O'Riordan (Genzyme, Framingham, MA), whereas Fischer rat thyroid cells were a generous gift of Drs. L. J. V. Galietta and O. Zegarra-Moran (Istituto Giannina Gaslini, Genova, Italy). Other cells and the vaccinia virus expression plasmid pTM1-CFTR4-expressing CFTR mutants were generous gifts of Professor M. J. Welsh (University of Iowa, Iowa City, IA). Cells were cultured and used as described (14–16, 19).

Electrophysiology—CFTR Cl^- channels were recorded in excised inside-out membrane patches using an Axopatch 200A patch-clamp amplifier and pCLAMP software (both from MDS Analytical Technologies, Union City, CA) as described (20).

The pipette (extracellular) solution contained 140 mM *N*-methyl-D-glucamine, 140 mM aspartic acid, 5 mM $CaCl_2$, 2 mM $MgSO_4$, and 10 mM TES, pH 7.3, with Tris ([Cl^-], 10 mM). The control bath (intracellular) solution contained 140 mM *N*-methyl-D-glucamine, 3 mM $MgCl_2$, 1 mM CsEGTA, 5 mM Tris, and 5 mM Bis-Tris, pH 7.3, with HCl ([Cl^-], 147 mM; free [Ca^{2+}], $<10^{-8}$ M) and was maintained at 37 °C; voltage was −50 mV. To ensure that the Cl^- concentration of different intracellular solutions was identical, all solutions were first titrated to pH 7.3 with HCl before we added either H_2SO_4 to titrate pH to acidic values or Tris/NaOH to titrate to alkaline values. By using Bis-Tris (pK_a 6.5) and Tris (Trizma® base; pK_a 8.1) instead of TES (pK_a 7.5) as the biological buffer, we buffered intracellular solutions over a wide range of pH_i values (pH_i 5.8–8.8).

After excision of inside-out membrane patches, we added PKA (75 nM) and ATP (1 mM) to the intracellular solution within 5 min of patch excision to activate CFTR. Once CFTR Cl^- channels were fully activated, we varied the pH_i value and/or [ATP] of the intracellular solution depending on the experimental protocol. Because MgATP controls CFTR channel gating (*e.g.* Refs. 21 and 22), we maintained the [MgATP] constant in different pH_i solutions by adding different amounts of Na_2ATP (for further information, see supplemental "Experimental Procedures" and Table 1). To minimize the rundown of CFTR Cl^- channels in excised membrane patches, we added PKA to all intracellular solutions. However, for studies of some CFTR constructs and wild-type CFTR in the absence of Mg^{2+} ions, it was also necessary to increase the [ATP] to 1 or 3 mM, respectively, to sustain channel activity.

To investigate how pH_i modulates CFTR Cl^- currents, we used membrane patches containing large numbers of active channels. For all other studies, we used membrane patches containing ≤5 active channels. We determined the number of channels in a membrane patch from the maximum number of simultaneous channel openings observed during the course of an experiment. To minimize errors when counting the number of active channels, we employed the strategies described by Cai *et al.* (14). For further information, see supplemental "Experimental Procedures." In all experiments, intracellular solutions titrated to different pH_i values were compared with the average of pre- and postintervention control periods titrated to pH_i 7.3, which contained the same concentrations of MgATP (or Mg^{2+}-free ATP) and PKA.

To investigate the effects of voltage on the CFTR Cl^- channel at different pH_i, we bathed membrane patches in symmetrical Cl^--rich solutions (extracellular pH (pH_e) 7.3; pH_i 7.3, 8.3, 8.8, or 6.3). From a holding voltage of −50 mV, we stepped voltage from −120 to +80 mV in 20-mV increments of 30 s. At each test voltage, we measured the single-channel current amplitude (i) and open probability (P_o) of CFTR (see below). We calculated the OH^- ion concentration ([OH^-]) of different intracellular solutions directly from pH_i values (pH_i 7.3, [OH^-] = 0.2 μM; pH_i 8.3, [OH^-] = 2 μM; pH_i 8.8, [OH^-] = 6.3 μM).

CFTR Cl^- currents were initially recorded on digital audiotape using a digital tape recorder (Biologic Scientific Instruments, model DTR-1204; Intracel Ltd., Royston, UK) at a bandwidth of 10 kHz. On playback, records were filtered with an eight-pole Bessel filter (model 902LPF2; Frequency Devices, Inc., Ottawa, IL) at a corner frequency of 500 Hz and acquired using a Digidata 1200 interface (MDS Analytical Technologies) and pCLAMP at sampling rates of 2.5 kHz (macroscopic currents) or 5 kHz (single-channel currents). For the purpose of illustration, current records were filtered at 500 Hz and digitized at 1 kHz.

To analyze the effects of pH_i on CFTR Cl^- currents, we determined the average CFTR Cl^- current (I^{CFTR}) at a specific pH_i by averaging all the data points collected at that pH_i and subtracting basal currents recorded in the absence of ATP and PKA. To plot the relationship between pH_i or [H_i^+], and CFTR Cl^- current, current values at different pH_i or [H_i^+] were ex-

pressed as a percentage of the control CFTR Cl^- current recorded at pH_i 7.3. To measure *i*, Gaussian distributions were fit to current amplitude histograms.

For NP_o, P_o, and burst analyses, lists of open and closed times were created using a half-amplitude crossing criterion for event detection as described under supplemental "Experimental Procedures." Burst analysis was performed as described by Carson *et al.* (16) using membrane patches that contained a single active channel and a t_c (the time that separates interburst closures from intraburst closures) determined from analyses of closed time histograms (supplemental Table 2). The mean interburst interval (IBI or T_{IBI}) was calculated using Equation 1,

$$P_o = T_b/(T_{MBD} + T_{IBI}) \quad \text{(Eq. 1)}$$

where T_b = (mean burst duration) × (open probability within a burst). Mean burst duration (MBD or T_{MBD}) and open probability within a burst ($P_{o(burst)}$) were determined directly from experimental data using pCLAMP software. P_o was calculated from open and closed times as described (23). However, for G551D and G1349D, because the number of active channels in a membrane patch was unknown, we measured NP_o instead of P_o.

To calculated the apparent voltage-dependent dissociation constant (K_d) for OH^- ion inhibition of CFTR and estimate the location of the binding site for OH^- ions within the CFTR pore, we employed the methods described by Sheppard and Robinson (20). For further information, see supplemental "Experimental Procedures."

Reagents—With the exception of PKA purified from bovine heart (Promega, Southampton, UK), chemicals were purchased from Sigma-Aldrich (Gillingham, UK). Stock solutions of ATP were prepared immediately before each experiment. When studying CFTR channel gating at ATP = 10 mM, we added $MgSO_4$ (7 mM) to the intracellular solution. For nominally Mg^{2+}-free intracellular solutions, we omitted $MgCl_2$ (3 mM) from the intracellular solution, titrated to pH 7.3 with HCl, and added EDTA (1 mM) to buffer free [Mg^{2+}] to <6 nM (22) before adjusting pH_i to 6.3 with H_2SO_4 and to pH 7.3 and 8.3 with Tris.

Statistics—Results are expressed as means ± S.E. of *n* observations. To compare sets of data, we used Student's *t* test. Differences were considered statistically significant when $p < 0.05$.

RESULTS

Multiple Effects of pH_i on CFTR Activity—To investigate whether pH_i regulates directly the CFTR Cl^- channel, we studied CFTR Cl^- currents in membrane patches excised from C127 cells expressing wild-type human CFTR. After CFTR activation by PKA-dependent phosphorylation at pH_i 7.3, we varied pH_i over the range pH_i 5.8 to 8.8 and recorded CFTR Cl^- currents while keeping the MgATP and PKA concentrations constant (for further information, see supplemental "Experimental Procedures" and Table 1. Fig. 1*A* demonstrates that changing pH_i altered the magnitude of CFTR Cl^- current in a readily reversible manner. At acidic pH_i, CFTR Cl^- currents were enhanced robustly at pH_i 6.8 and 6.3, but decreased at pH_i 5.8 (Fig. 1*B*). By contrast, at alkaline pH_i, CFTR Cl^- currents

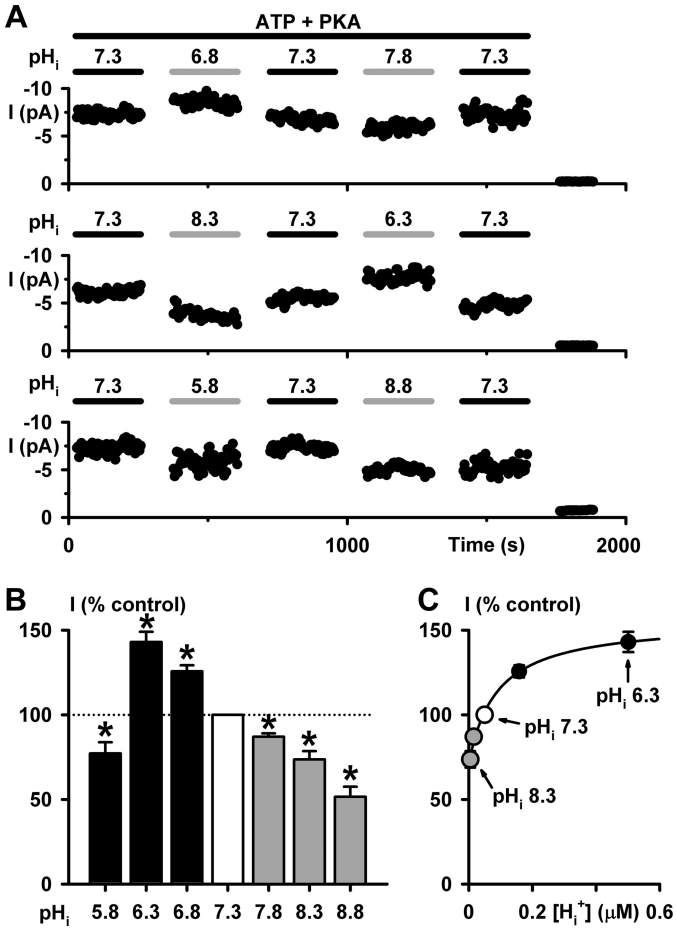

FIGURE 1. **pH_i modulates CFTR Cl^- current.** *A*, time courses of wild-type CFTR Cl^- current in excised inside-out membrane patches. In this and subsequent figures, unless otherwise indicated, ATP (0.3 mM) and PKA (75 nM) were continuously present in intracellular solutions, which were adjusted to the indicated pH_i; voltage was −50 mV, and there was a large Cl^- concentration gradient across the membrane ($[Cl^-]_{int}$, 147 mM; $[Cl^-]_{ext}$, 10 mM). For the purpose of illustration, time courses have been inverted, and *upward deflections* represent inward currents. *B*, effects of pH_i on CFTR Cl^- currents. Data are means ± S.E. ($n = 6$) expressed as a percentage of the control current at pH_i 7.3. The *asterisks* indicate values that are significantly different from the control ($p < 0.05$). *C*, relationship between intracellular proton concentration ($[H_i^+]$) and CFTR activity. Data from *B* are plotted *versus* $[H_i^+]$. The continuous line is the fit of a hyperbolic function to the mean data ($y = y_0 + ax/(b + x)$, where $y_0 = 70.9$, $a = 84.7$, and $b = 8.8 \times 10^{-8}$; $r = 0.99$). *Error bars* are smaller than symbol size except where shown.

decreased steadily (Fig. 1*B*). To examine the pH_i sensitivity of CFTR, we explored the relationship between CFTR Cl^- current and the proton concentration ($[H^+]$) of pH_i solutions. Over the pH_i range pH_i 6.3–8.3, the data were best fit by a hyperbolic function with a half-maximal stimulatory concentration (K_s) at pH_i 7.06 (Fig. 1*C*). We interpret these data to suggest that CFTR activity is regulated by pH_i and that this regulation involves the protonation of CFTR.

In principle, pH_i might alter CFTR Cl^- current in one or more of three ways: (i) by regulating the number of active channels (*N*), (ii) by modulating current flow through open channels, and (iii) by controlling channel gating and, hence, P_o. To understand how pH_i regulates CFTR, we investigated the effects of pH_i on the single-channel activity of CFTR. Fig. 2 shows representative recordings of a single wild-type CFTR Cl^- channel at different pH_i. Visual inspection of these records

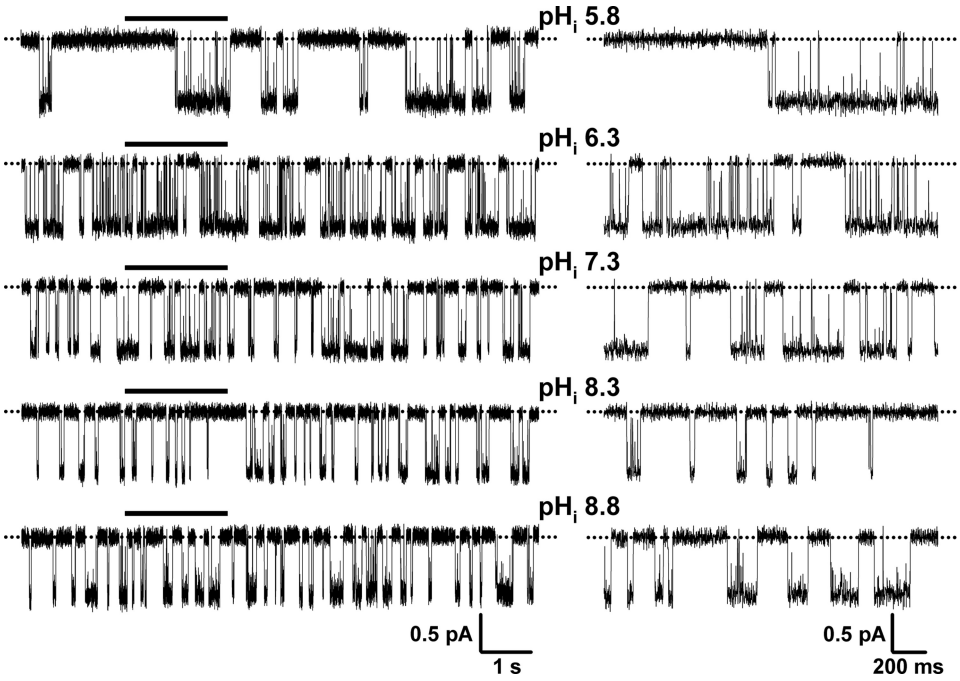

FIGURE 2. **The single channel activity of wild-type CFTR at different pH_i.** Representative recordings show the activity of a single wild-type CFTR Cl^- channel at different pH_i. *Dotted lines* indicate where the channel is closed, and *downward deflections* correspond to channel openings. The 2-s portions indicated by *bars* are shown on an expanded time scale to the *right* of each 10-s recording.

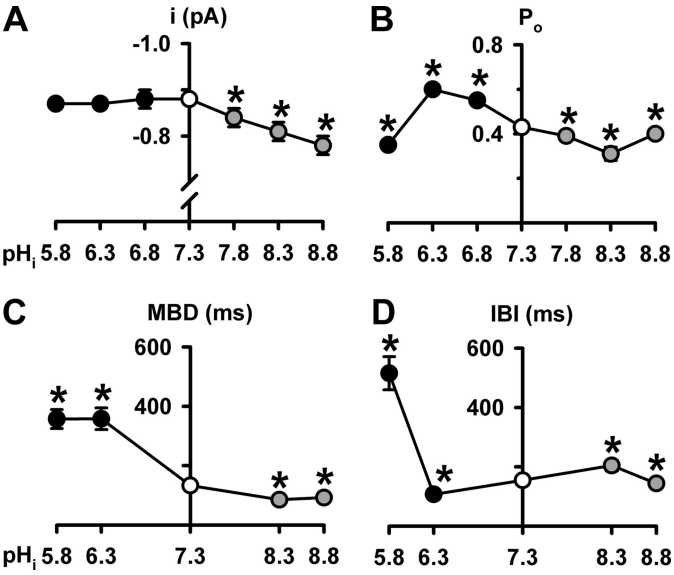

FIGURE 3. **pH_i alters the single-channel activity of CFTR.** *A–D*, single channel current amplitude (*i*), open probability (P_o), mean burst duration (MBD), and interburst interval (IBI) of wild-type CFTR at different pH_i values. Data are means ± S.E. (n = 4–14). The *asterisks* indicate values that are significantly different from the control value ($p < 0.05$). Note the break in the *ordinate* in *A*.

suggests that varying pH_i had striking effects on CFTR channel gating, little effect on single-channel current amplitude (*i*), and none on *N*. However, when we measured *i*, we found that *i* was unaltered at acidic pH_i but diminished progressively at alkaline pH_i (Fig. 3*A*), suggesting that OH^- ions inhibit the CFTR Cl^- channel.

The pattern of gating of wild-type CFTR at pH_i 7.3 is characterized by bursts of channel openings interrupted by brief flickery closures and separated by longer closures between bursts (*e.g.* Ref. 24 and Fig. 2, *third trace from the top*). To quantify the pH_i dependence of channel gating, we measured P_o and performed an analysis of bursts. Over the pH_i range pH_i 6.3–8.3, P_o decreased steadily as pH_i increased (Fig. 3*B*). However, between pH_i 6.3 and 5.8, P_o fell sharply, whereas between pH_i 8.3 and 8.8, it rose, returning to a value similar to that of pH_i 7.8 (Fig. 3*B*). At acidic pH_i, MBD increased dramatically, whereas at alkaline pH_i, MBD decreased (Fig. 3*C*). By contrast, Fig. 3*D* demonstrates that the relationship between pH_i and IBI is complex. At acidic pH_i, IBI decreased at pH_i 6.3, but increased markedly at pH_i 5.8, whereas at alkaline pH_i, IBI increased at pH_i 8.3, but was unchanged at pH_i 8.8 (Fig. 3*D*). Thus, pH_i has intricate effects on CFTR channel gating. However, the effects of pH_i on the single-channel behavior of CFTR account for the pH_i dependence of CFTR Cl^- currents (supplemental Table 3). Based on the control experiments described under supplemental "Results", we suggest that pH_i regulates directly the CFTR Cl^- channel.

OH^- Ions Occlude the CFTR Pore—Fig. 3*A* demonstrates that the *i* of CFTR diminishes progressively with alkalinization of the intracellular solution, suggesting that OH^- ions might inhibit the CFTR Cl^- channel by acting as an open-channel blocker (25). To test this hypothesis, we investigated the effects of membrane voltage on the *i* of wild-type CFTR at alkaline pH_i. We reasoned that negative voltages would drive OH^- ions from the intracellular solution into the CFTR Cl^- channel where they might bind, occlude the channel pore, and block Cl^- permeation. Conversely, positive voltages would drive Cl^- ions into the CFTR Cl^- channel from the extracellular solution, flushing blocking OH^- ions from the channel pore and relieving inhibition.

Fig. 4*A* shows representative recordings of a single CFTR Cl^- channel at −80 and +80 mV, Fig. 4*B* shows the single-channel current-voltage (*I-V*) relationship of wild-type CFTR at pH_i 7.3 and 8.3, and Fig. 4*C* shows the voltage dependence of the fraction of *i* inhibited at pH_i 8.3. Fig. 4, *A–C*, demonstrates that at negative voltages there was a small, but significant, decrease in the *i* of wild-type CFTR at pH_i 8.3 compared with that at pH_i 7.3. By contrast, at positive voltages the inhibition of *i* was completely relieved (Fig. 4, *A–C*) (similar results were observed at pH_i 8.8 over the voltage range −80 to +80 mV (data not shown)). Block of *i* at negative voltages, but relief at positive voltages suggests that OH^- ions occlude the intracellular vestibule of the CFTR pore.

To determine the potency with which OH^- ions block the CFTR pore, we calculated the apparent voltage-dependent dissociation constant (K_d) for OH^- ion inhibition of wild-type

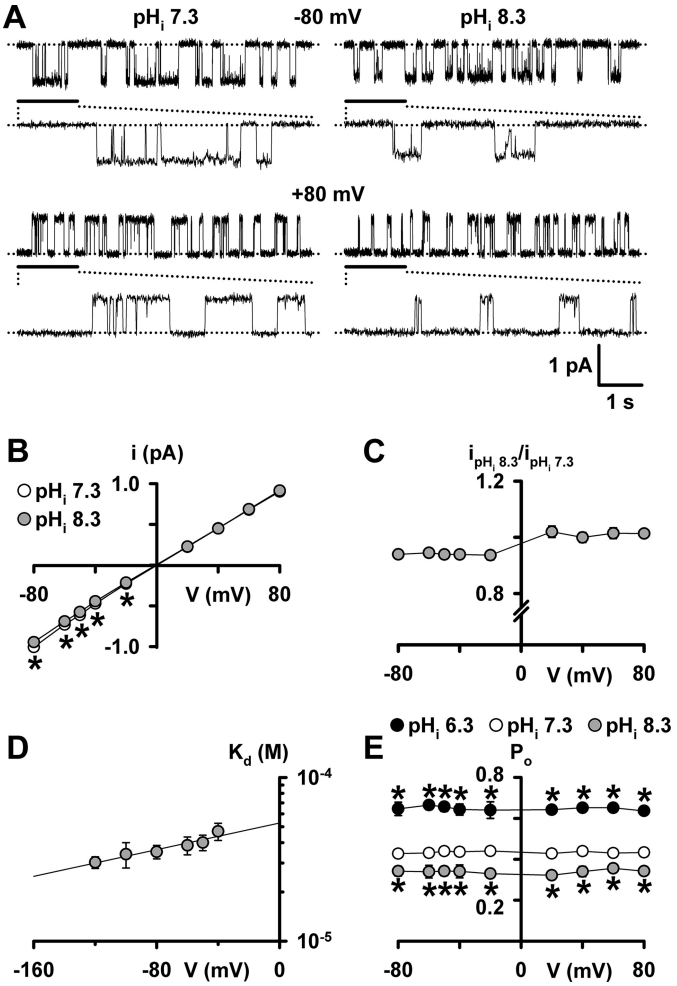

FIGURE 4. **Voltage-dependent inhibition of current flow through the CFTR pore by OH^- ions.** *A*, representative recordings show the effects of alkalinizing the intracellular solution to pH_i 8.3 on the activity of a single wild-type CFTR Cl^- channel at −80 mV (*top*) and +80 mV (*bottom*). The recording conditions were identical to those used in Figs. 1 and 2 with the exception that the membrane patch was bathed in symmetrical 147 mM Cl^- solutions. *Dotted lines* indicate where the channel is closed, and *downward deflections* at −80 mV and *upward deflections* at +80 mV correspond to channel openings. The 1-s portions indicated by *bars* are shown on an expanded time scale *below* each 5-s recording. *B*, single-channel current-voltage (*I-V*) relationships of wild-type CFTR at pH_i 7.3 (*white circles*) and pH_i 8.3 (*gray circles*) using the conditions described in *A*. *C*, voltage dependence of the fraction of *i* inhibited at pH_i 8.3. *D*, relationship between the voltage-dependent dissociation constant (K_d) and voltage at alkaline pH_i (pH_i 8.3 and pH_i 8.8). *E*, voltage dependence of P_o at pH_i 6.3, pH_i 7.3, and pH_i 8.3. Data are means ± S.E. (*B*, *C*, and *E*, $n = 6$; *D*, $n = 3$–9, except −120 mV, where $n = 2$). In *B* and *D*, the continuous lines are the fits of first-order regression functions to the data. In *B* and *E*, the *asterisks* indicate values that are significantly different from the control ($p < 0.05$). *Error bars* are smaller than symbol size except where shown.

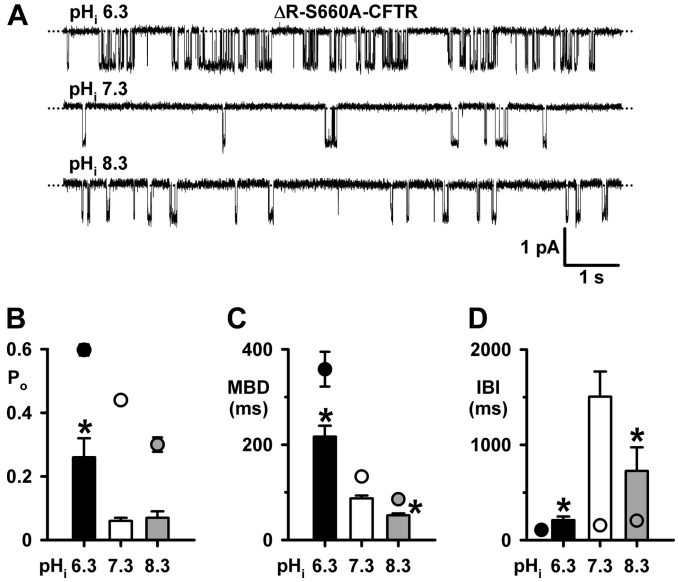

FIGURE 5. **Acidic pH_i potentiates the activity of ΔR-S660A-CFTR.** *A*, representative recordings show the effects of pH_i on the activity of a single ΔR-S660A-CFTR Cl^- channel. *Dotted lines* indicate where the channel is closed, and *downward deflections* correspond to channel openings. *B*, *C*, and *D*, effects of pH_i on the P_o, MBD, and IBI of ΔR-S660A (*columns*) and wild-type CFTR (*circles*). Data are means ± S.E. (*B*, $n = 6$ for all data; *C* and *D*, ΔR-S660A-CFTR, $n = 3$; wild-type-CFTR, $n \geq 6$); *asterisks* indicate ΔR-S660A-CFTR values that are significantly different from the pH_i 7.3 control ($p < 0.05$).

CFTR. Fig. 4*D* demonstrates that apparent K_d(V) values for CFTR inhibition by OH^- ions are weakly voltage-dependent. The data also indicate that the potency of CFTR inhibition by OH^- ions (apparent K_d (0 mV) = 54 ± 6 μM; $n = 9$) approaches that of the best-studied CFTR blocker, the sulfonylurea glibenclamide (K_d (0 mV) = 37 μM) (20).

To estimate the location of the binding site for OH^- ions within the CFTR pore, we calculated the electrical distance across the membrane sensed by OH^- ions using the Woodhull equation (26), as described under supplemental "Experimental Procedures." Using the data in Fig. 4*D* and assuming a single binding site for OH^- ions, $z' = 0.23 \pm 0.03$ ($n = 9$), measured from the inside of the membrane over the voltage range −120 to −40 mV. These data suggest that the penetration of OH^- ions into the transmembrane electric field from the intracellular side is 23%, similar to that of SCN^- ions (20%) (27). Thus, at alkaline pH_i, OH^- ions cause open-channel block of the CFTR Cl^- channel by occupying a superficial site within the intracellular vestibule of the CFTR pore.

In contrast to the effects of pH_i on *i* (Figs. 3*A* and 4, *B* and *C*), the pH_i dependence of P_o was voltage-independent (Fig. 4*E*). At all voltages tested, the P_o of wild-type CFTR was diminished at pH_i 8.3, but augmented at pH_i 6.3. The data also suggest that inhibition of CFTR Cl^- current at alkaline pH_i results predominantly from a diminution of P_o rather than a decrease in *i* (supplemental Table 3).

pH_i Modulates the Function of the NBDs and RD—CFTR channel gating is controlled by the NBDs and RD (2, 3). Therefore, we reasoned that pH_i might modulate CFTR activity by altering the function of these domains. To test this hypothesis, we adopted two strategies; first, we employed the CFTR construct ΔR-S660A that deletes a large part of the RD and is not regulated by PKA-dependent phosphorylation (13) to explore separately how pH_i influences the function of the RD and NBDs. Second, we investigated the effects of pH_i on the ATP dependence of CFTR channel gating. For these experiments, we studied CFTR potentiation at pH_i 6.3 and CFTR inhibition at pH_i 8.3.

Fig. 5*A* shows representative recordings of a single ΔR-S660A-CFTR Cl^- channel at different pH_i, whereas Fig. 5, *B*–*D* quantifies the effects of pH_i on channel gating. Consistent with previous studies (13), at pH_i 7.3 the P_o of ΔR-S660A-CFTR was attenuated markedly compared with that of wild-type CFTR

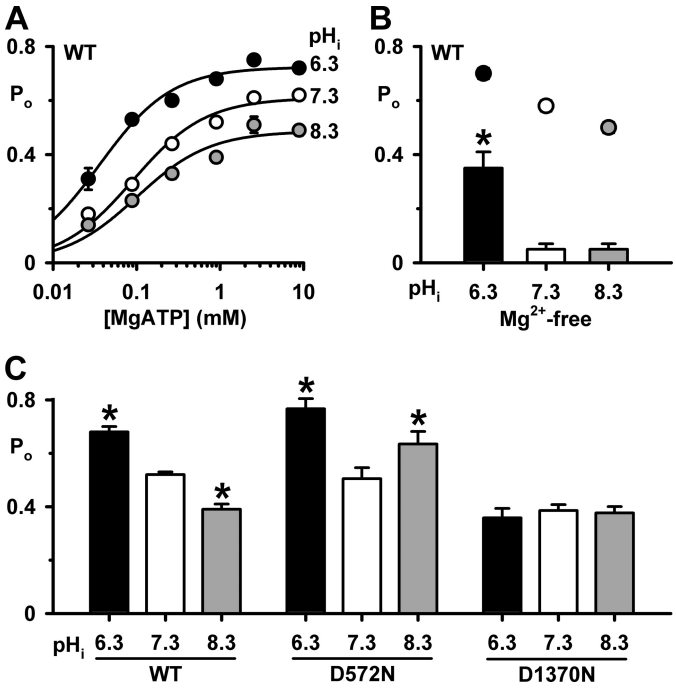

FIGURE 6. **pH_i modulates the MgATP dependence of CFTR channel gating.** *A*, relationship between [MgATP] and P_o of wild-type CFTR at the indicated pH_i values. The *continuous lines* are Michaelis-Menten fits to mean data. *B* and *C*, effects of pH_i on the P_o of wild-type (*WT*), D572N-, and D1370N-CFTR in the presence of ATP (3 mM in *B* or 1 mM in *C*). In *B*, wild-type CFTR data were acquired in the presence (*circles*) and absence (*columns*) of Mg^{2+} (3 mM), whereas in *C*, wild-type, D572N-, and D1370N-CFTR data were acquired in the continuous presence of Mg^{2+} (3 mM). All data are means ± S.E. (n = 5–7); *asterisks* indicate values that are significantly different from the control value ($p < 0.05$).

because its MBD was reduced 0.4-fold, while its IBI was prolonged 9-fold (Fig. 5, *B–D*). Acidifying to pH_i 6.3 potentiated the P_o of wild-type CFTR 0.4-fold, but that of ΔR-S660A-CFTR 3.3-fold (Fig. 5*B*). Fig. 5, *C* and *D*, demonstrates that the marked potentiation of ΔR-S660A-CFTR P_o at pH_i 6.3 was primarily caused by a 0.9-fold decrease in IBI, but it was also enhanced by a 1.5-fold increase of MBD. Alkalinizing to pH_i 8.3 decreased the P_o of wild-type CFTR 0.3-fold, but was without effect on the P_o of ΔR-S660A-CFTR (Fig. 5*B*). An explanation for this striking difference between wild-type and ΔR-S660A-CFTR is shown in Fig. 5*D*. Between pH_i 7.3 and 8.3, the IBI of wild-type CFTR increased 0.3-fold, whereas that of ΔR-S660A-CFTR decreased 0.5-fold (Fig. 5*D*). Fig. 5*D* also reveals that the relationship between IBI and pH_i is linear for wild-type CFTR, but bell-shaped for ΔR-S660A-CFTR over the pH_i range 6.3–8.3. We interpret the failure of pH_i 8.3 to attenuate ΔR-S660A-CFTR channel gating to suggest that alkaline pH_i might inhibit CFTR channel gating, at least in part, by modulating RD function. However, the robust potentiation of ΔR-S660A-CFTR channel gating at pH_i 6.3 argues that acidic pH_i likely enhances CFTR channel gating by acting on sites distinct from the RD.

To investigate whether pH_i influences NBD function, we studied the ATP dependence of CFTR channel gating. Fig. 6*A* shows the relationship between [MgATP] and P_o for wild-type CFTR at pH_i 6.3, 7.3, and 8.3. At each pH_i tested, as the [MgATP] increased, P_o values enlarged. However, altering pH_i influenced both the MgATP sensitivity and channel activity of wild-type CFTR (Fig. 6*A*). These differences are best illustrated by considering values of K_D (the [MgATP] required for half-maximal P_o, which describes the apparent affinity of CFTR for MgATP) and $P_{o\ max}$ (the maximum P_o) determined from Michaelis-Menten fits to the mean data (pH_i 6.3: $K_D = 36 \pm 5$ μM, $P_{o\ max} = 0.72 \pm 0.01$, $r^2 = 0.99$; pH_i 7.3: $K_D = 90 \pm 14$ μM, $P_{o\ max} = 0.61 \pm 0.02$, $r^2 = 0.99$; pH_i 8.3: $K_D = 100 \pm 24$ μM, $P_{o\ max} = 0.49 \pm 0.02$, $r^2 = 0.97$; Fig. 6*A*). Two conclusions are apparent from these data. First, acidifying pH_i enhances markedly the apparent MgATP affinity of CFTR, whereas alkalinizing pH_i has little effect. Second, acidifying pH_i augments channel activity, whereas alkalinizing pH_i inhibits CFTR.

The Role of Mg^{2+} Ions in Determining the pH_i Sensitivity of the NBDs—Mg^{2+} ions are a pre-requisite for the hydrolysis of ATP that drives CFTR channel closure (21, 22). To learn whether pH_i modulates CFTR channel gating by affecting the interaction of Mg^{2+} ions with the NBDs, we examined the single-channel activity of CFTR in the absence of Mg^{2+} ions at different pH_i (Figs. 6*B* and supplemental Fig. 3*A*). At pH_i 7.3 removal of Mg^{2+} ions attenuated markedly the P_o of CFTR (Fig. 6*B*). Nevertheless, acidification to pH_i 6.3 enhanced strongly P_o, whereas alkalinization to pH_i 8.3 was without effect (Fig. 6*B*). These data suggest that the presence of Mg^{2+} ions is critical for the inhibition of CFTR channel gating at alkaline pH_i. By contrast, the potentiation of CFTR channel gating at pH_i 6.3 is both dependent on, and independent of, Mg^{2+} ions.

To understand better the role of Mg^{2+} ions in determining the pH_i sensitivity of the NBDs, we studied Asp-572 and Asp-1370, the Walker B aspartates that coordinate Mg^{2+} ions in ATP binding sites 1 and 2 of the ATP-driven NBD dimerization model of CFTR channel gating (3, 28). Previous studies have demonstrated that the mutations D572N- and D1370N-CFTR abolish Mg^{2+} binding to the NBDs (21, 22). Figs. 6*C* and 8 and supplemental Fig. 3, *B* and *C*, demonstrate that the gating behavior of D572N- and D1370N-CFTR Cl^- channels at different pH_i diverges from that of wild-type CFTR in several important respects. First, at pH_i 7.3, the P_o of D572N-CFTR was the same as wild-type CFTR, whereas that of D1370N-CFTR was reduced (Fig. 6*C*). Second, at pH_i 6.3, the P_o of D572N-CFTR was potentiated markedly because IBI was decreased 0.7-fold and MBD was increased 1.4-fold (Figs. 6*C* and 8 and supplemental Fig. 3*B*). By contrast, for D1370N-CFTR at pH_i 6.3, gating behavior and, hence, P_o were unchanged (Fig. 6*C* and supplemental Fig. 3*C*). Third, in striking contrast to wild-type CFTR, at pH_i 8.3 D572N-CFTR channel gating was enhanced because MBD was increased 0.6-fold and IBI decreased 0.3-fold, whereas that of D1370N-CFTR was unaltered (Figs. 2 and 8 and supplemental Fig. 3, *B* and *C*). As a result, at pH_i 8.3, the P_o of wild-type CFTR decreased, that of D1370N-CFTR was unchanged, whereas that of D572N-CFTR increased (Fig. 6*C*).

Several conclusions can be drawn from the data in Fig. 6*C*. First, the potentiation of D572N-CFTR channel activity at pH_i 8.3 suggests that the binding of Mg^{2+} ions at site 1 is essential for the inhibition of CFTR channel gating at alkaline pH_i. Second the lack of effect of pH_i on D1370N argues that the pH_i sensitivity of CFTR channel gating is dependent on Mg^{2+} binding to site 2. This suggests that pH_i might exert its effects on CFTR channel gating by altering the ATPase activity of site 2.

ATP Binding Site 2 Is a Crucial Determinant of the pH_i Sensitivity of CFTR Channel Gating—Structural (29–32) and functional (16, 21) studies suggest that the phosphate groups of ATP are key determinants of ATP binding to sites 1 and 2. The Walker A lysine residues Lys-464 (site 1) and Lys-1250 (site 2), which bind the γ-phosphate of ATP, are highly conserved and critical for ATP binding and hydrolysis (16, 21, 29). Moreover, the LSGGQ motifs contain the highly conserved glycine residues Gly-551 (site 2) and Gly-1349 (site 1) that clamp the phosphate tail of ATP during ATP-driven NBD dimerization (29, 30, 32). Of note, the CF mutations G551D and G1349D perturb severely CFTR channel gating (14, 33). Using CFTR constructs bearing site-directed mutations, we examined the roles of the residues Lys-464, Lys-1250, Gly-551, and Gly-1349 in determining the pH_i sensitivity of CFTR channel gating.

Consistent with previous studies (14, 33), G1349D-CFTR and especially G551D-CFTR attenuated strongly CFTR channel gating at pH_i 7.3, with brief, poorly resolved channel openings separated by very long-lasting closures (Fig. 7, *A* and *C*). Fig. 7, *A–D*, demonstrates that the gating behavior and, hence, NP_o of G551D- and G1349D-CFTR were unaffected by pH_i. Because tight dimerization of the NBDs is a prerequisite for channel opening (28) and because G551D and G1349D perturb severely channel gating (14, 33), we speculate that the effects of pH_i on CFTR channel gating are dependent on the formation of an NBD1:NBD2 dimer.

Fig. 7, *E* and *G*, show the hallmark effects of mutating the Walker A lysines in NBD1 and NBD2 on CFTR channel gating (16, 21). At pH_i 7.3, bursts of K464A-CFTR channel openings were separated by prolonged channel closures, whereas dramatically prolonged bursts of K1250M-CFTR channel openings were separated by very long-lived channel closures (Figs. 7, *E* and *G*, and 8). Although P_o values of K464A-CFTR were less than those of wild-type CFTR at all pH_i values tested, the effects of acidic and alkaline pH_i on K464A- and wild-type CFTR were similar (Fig. 7, *E* and *F*). This suggests that K464A-CFTR does not change the pH_i sensitivity of CFTR. By contrast, the pH_i sensitivity of K1250M-CFTR differed strikingly from that of wild-type CFTR. At pH_i 6.3, the P_o of K1250M-CFTR was reduced because MBD was decreased 0.7-fold, whereas IBI was unchanged (Figs. 7, *G* and *H*, and 8). At pH_i 8.3, the P_o of K1250M-CFTR was increased, albeit slightly, as a result of a small increase in MBD and no change in IBI (Figs. 7*H* and 8). Fig. 7*H* also reveals that the P_o of K1250M-CFTR was similar to that of wild-type CFTR at pH_i 8.3, but greatly diminished at pH_i 7.3 and 6.3. Thus, the pH_i sensitivity of K1250M-CFTR is the converse of that of wild-type CFTR.

Taken together, our data argue that ATP binding site 2 is a crucial determinant of the pH_i sensitivity of the CFTR Cl^- channel. They also suggest that MgATP binding at site 1 might be important for mediating the inhibitory effects of alkaline pH_i and cooperating with site 2 to drive channel gating.

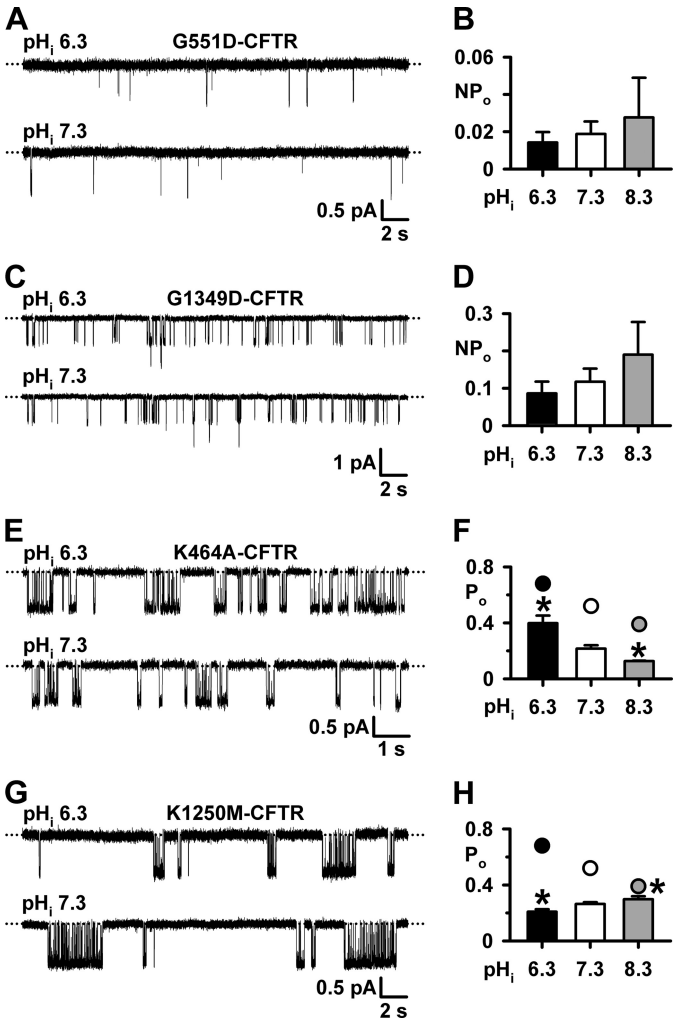

FIGURE 7. **Role of ATP phosphate binding in CFTR regulation by pH_i.** *A*, *C*, *E*, and *G*, representative recordings show the effects of pH_i on the activity of G551D-, G1349D-, K464A-, and K1250M-CFTR Cl^- channels in the presence of ATP (1 mM). *Dotted lines* indicate where channels are closed, and *downward deflections* correspond to channel openings. *B*, *D*, *F*, and *H*, effects of pH_i on the NP_o of G551D- and G1349D-CFTR and P_o of K464A- and K1250M-CFTR. Data are means ± S.E. ($n = 6$, except G551D- and G1349D-CFTR at $pH_i = 8.3$, where $n = 3$). The *asterisks* indicate values that are significantly different from the control value ($p < 0.05$). In *F* and *H*, wild-type CFTR data (*circles*) are shown for comparison.

DISCUSSION

In this study we investigated whether pH_i regulates directly CFTR activity and the responsible mechanisms. Our data demonstrate that acidic pH_i stimulates CFTR Cl^- currents by potentiating channel gating, whereas alkaline pH_i attenuates CFTR Cl^- currents predominantly by inhibiting channel gating, but also by obstructing Cl^- flow through the CFTR pore. Using CFTR constructs, we demonstrate that ATP-binding site 2 is a primary determinant of the pH_i sensitivity of CFTR. Our data suggest that the mechanism by which pH_i regulates CFTR is distinct from other ion channels. Instead of protons modifying channel gating by interacting with residues within (*e.g.* ClC-0 (34)) or close to the intracellular vestibule (*e.g.* Kir1.1 (35)) of the channel pore, in CFTR protons modulate channel gating by altering the function of ATP-binding site 2 in the NBDs.

Molecular Mechanisms of CFTR Regulation by pH_i—Our data demonstrate that pH_i has multiple effects on the CFTR Cl^- channel. They also reveal that pH_i modulates CFTR function by altering the activity of each of the domains from which CFTR is assembled. In Fig. 9 we summarize the molecular mechanisms by which pH_i regulates current flow through

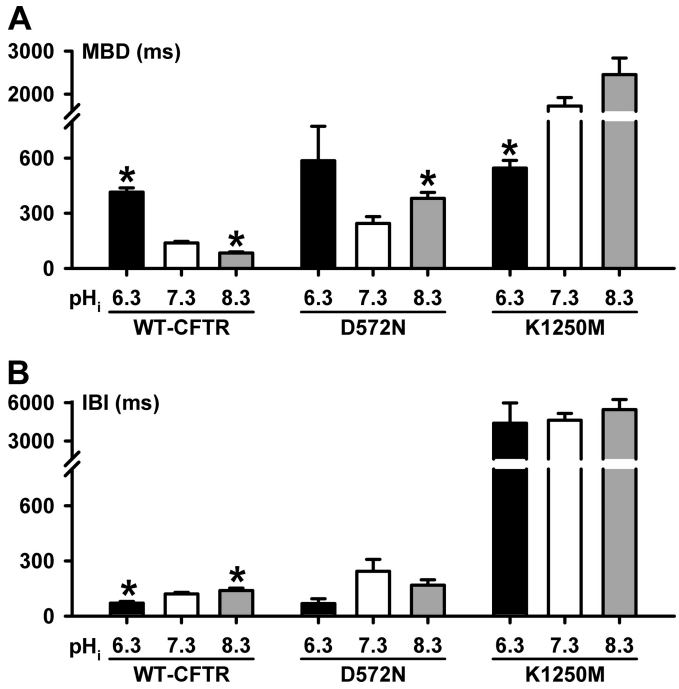

FIGURE 8. **Burst analysis of D572N- and K1250M-CFTR.** *A* and *B*, MBD and IBI of D572N- and K1250M-CFTR at different pH_i values; wild-type CFTR data are shown for comparison. Data are means ± S.E. (D572N- and K1250M-CFTR, $n = 3$; wild-type-CFTR, $n \geq 6$). The *asterisks* indicate values that are significantly different from the pH_i 7.3 control ($p < 0.05$). Note the breaks in the *ordinates*.

the CFTR pore and the control of channel gating by the NBDs and RD.

OH^- ions inhibit CFTR function in several ways. First, OH^- ions are open-channel blockers of the CFTR pore that disrupt Cl^- flow by interacting with a superficial site within the intracellular vestibule of the CFTR pore. Second, studies of the CFTR construct ΔR-S660A suggest that OH^- ions might inhibit CFTR channel gating, at least in part, by modulating RD function. Third, OH^- ions inhibit CFTR function by regulating the control of channel gating by ATP-driven NBD dimerization (3, 21). The decrease in channel activity at alkaline pH_i argues that OH^- ions might destabilize ATP binding at sites 1 and 2, promoting dissociation of the NBD dimer and channel closure. However, our data also suggest that the binding of Mg^{2+} ions at site 1 is essential for CFTR inhibition by OH^- ions.

In contrast to the effects of OH^- ions, H^+ ions mediate their effects on CFTR predominantly by modulating the control of channel gating at the NBDs. Our studies argue that ATP-binding site 2 is a crucial determinant of the pH_i sensitivity of CFTR. The data suggest that H^+ ions enhance the affinity with which MgATP binds at site 2 and stabilize ATP binding at this site with the result that the frequency of channel openings is increased and their duration prolonged. Thus, pH_i regulates directly CFTR function. Importantly, this regulation occurs within the physiological pH_i range (36), consistent with previous work demonstrating a significant role for CFTR in the regulation of pH_i (*e.g.* Ref. 5, 6, 37, and 38).

Open-channel Block of the CFTR Pore by OH^- Ions—At negative voltages OH^- ions caused a small reduction of the *i* of CFTR. Given the low concentration of OH^- ions in our test solutions (see "Experimental Procedures"), the potency of OH^- ion inhibition of CFTR is surprisingly strong, exceeding that of many open-channel blockers of CFTR (*e.g.* diphenylamine-2-carboxylate and flufenamic acid (39)). Interestingly, the location of the OH^- ion-binding site within the transmembrane electric field (23%) is similar to that of SCN^- ions (20%) (27). These data argue that OH^- and SCN^- ions interact with a superficial site(s) within the intracellular vestibule of the CFTR pore (Fig. 9). The shallow penetrance of OH^- and SCN^- ions into the CFTR pore contrasts with that of large organic anions (*e.g.* glibenclamide (20)), which penetrate deep into the intracellular vestibule to interact with a site located halfway across the electric field of the membrane from the inside. Site-directed mutagenesis of Lys-95, located toward the extracellular end of the first transmembrane segment, reveals that the positive charge at Lys-95 is essential for channel block by glibenclamide and four other open-channel blockers of CFTR with unrelated chemical structures (40). However, studies of the kinetics of channel block (41–43) demonstrate that the interaction of open-channel blockers with CFTR is complex and likely to involve multiple binding sites within the intracellular vestibule of the CFTR pore. One of these binding sites might overlap with that of OH^- ions.

Intricate Effects of pH_i on CFTR Channel Gating—Our data reveal that pH_i has complex effects on CFTR channel gating. Over the pH_i range 6.3 to 8.3, the P_o of wild-type CFTR decreases steadily because of reciprocal changes in IBI and MBD. This suggests that between pH_i 6.3 and 8.3, the effects of pH_i on MBD and IBI are coordinated. By contrast, our data suggest that in strongly acidic and alkaline intracellular solutions, MBD values are stable, whereas those of IBI appear unstable.

At pH_i 5.8 the IBI of wild-type CFTR was prolonged strikingly, indicating that channel opening is very difficult at strongly acidic pH_i. At pH_i 5.8, $MgATP^{2-}$ is partially protonated at the γ-phosphate to become $MgHATP^-$ (44). This suggests that protonated ATP at pH_i 5.8 might interfere with the formation of H-bonds between CFTR and the γ-phosphate of ATP, attenuating ATP binding and impeding channel opening. However, we speculate that protonation of phosphate groups in other parts of the CFTR gating pathway or on the RD at strongly acidic pH_i might also contribute to this result.

Interestingly, at pH_i 8.8 the IBI of wild-type CFTR was attenuated with the result that the P_o of wild-type CFTR at pH_i 8.8 enlarged to become equivalent to that at pH_i 7.8. Because negative surface charge increases with alkalinization of the intracellular solution, the diminution of IBI at pH_i 8.8 might represent a change in RD conformation or the interaction of the RD with other domains of CFTR (Fig. 9). For example, manipulation of the surface charge on the RD might mimic the effects of RD phosphorylation and disrupt interactions between the RD and NBDs leading to channel activation (13, 45, 46). Alternatively, increased negative surface charge at alkaline pH_i might alter the balance between stimulatory and inhibitory RD phosphorylation sites to favor channel activation (47).

In contrast to the effects of strong alkaline pH_i on wild-type CFTR, our studies of the ΔR-S660A-CFTR Cl^- channel at pH_i 8.3 argue that alkaline pH_i inhibits CFTR channel gating, at

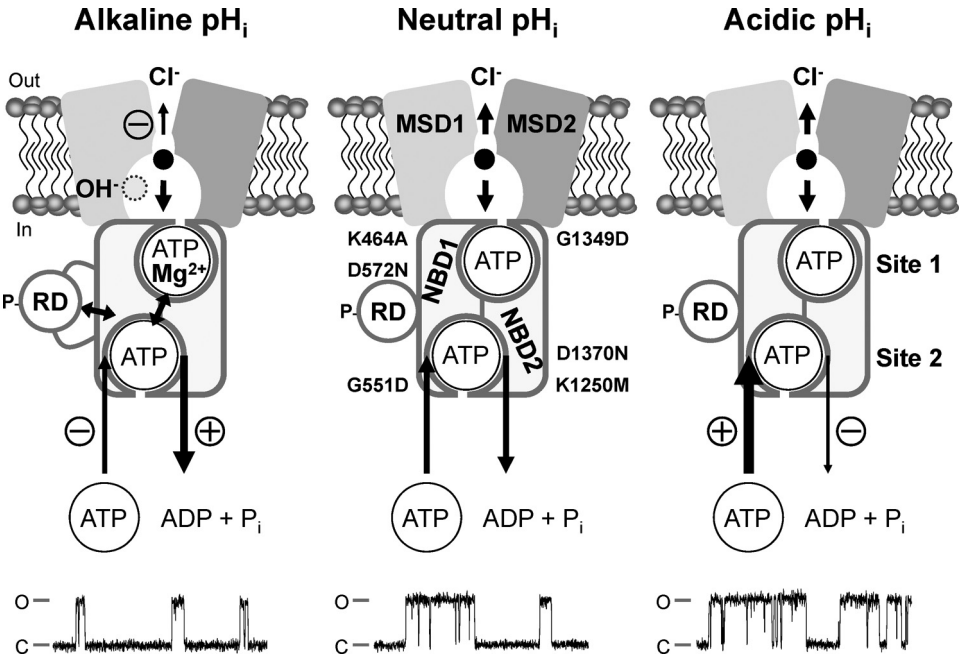

FIGURE 9. **Multiple mechanisms of CFTR regulation by pH_i.** The simplified models show an open CFTR Cl^- channel with a phosphorylated RD and NBDs assembled to form a head-to-tail dimer with ATP molecules bound at ATP binding sites 1 and 2. Each ATP binding site is formed by the Walker A and B motifs of one NBD and the LSGGQ motif of the other NBD. The locations of the site-directed mutations examined in this study are shown. The models show the direct effects of H^+ and OH^- ions on the function of the individual domains of CFTR at alkaline, neutral, and acidic pH_i. Single-channel recordings are shown *beneath each model*. For the purpose of illustration, the recordings have been inverted, and *upward deflections* correspond to channel openings. *MSD*, membrane-spanning domain; *P*, phosphorylation of the RD; P_i, inorganic phosphate. *In* and *Out* denote the intra- and extracellular sides of the membrane, respectively, whereas *C* and *O* indicate the closed and open-channel states, respectively. The *long arrows* represent the regulation of CFTR channel gating by ATP-driven NBD dimerization; *arrow thickness* and *symbols* indicate reaction speed (*thick* (+), fast (potentiation); *thin* (−), slow (inhibition)). *Double-headed arrows* denote interactions between the NBDs and RD and cross-talk between ATP-binding sites 1 and 2. *Short arrows* within the CFTR pore denote Cl^- ion flow; *arrow thickness* and *symbols* indicate ease of flow (*thick*, unobstructed; *thin* (−), obstructed). See "Discussion" and Refs. 2, 3, and 25 for further information.

least in part, by modulating RD function. The reason why ΔR-S660A-CFTR is not inhibited at pH_i 8.3 is that its prolonged IBI is attenuated, not extended, at this pH_i value. Further studies are required to understand the underlying mechanisms. However, it is interesting to note that for both ΔR-S660A-CFTR and the ATP-binding site 1 mutant D572N-CFTR, the relationship between pH_i and IBI is bell-shaped, not linear, between pH_i 6.3 and 8.3 (Figs. 5*D* and 8*B*). We interpret these data to suggest that the pH_i dependence of IBI reflects complex interactions between the RD and NBDs.

Use of the ATP-driven NBD Dimerization Model of CFTR Channel Gating to Explain the Effects of pH_i—Like other ABC transporters, the two NBDs of CFTR likely form a head-to-tail dimer that sandwiches ATP molecules within two binding sites (termed site 1 and site 2) located at the NBD1:NBD2 interface (3, 21). In CFTR, site 1 has no ATPase activity, but site 2 cyclically hydrolyzes ATP to drive channel gating (3, 21). In this asymmetric gating model, ATP-induced dimerization at site 1 likely occurs before that at site 2, which in turn precedes CFTR opening (48).

Structural studies of ABC transporters (29–32) demonstrate that within the ATP-binding sites the *cis* NBD anchors the phosphate tail of an ATP molecule by a network of hydrogen bonds (H-bonds) and hydrogen-mediated salt bridges from the Walker A motif. By contrast, in the *trans* NBD, only H-bonds from the LSGGQ motif clamp the γ-phosphate of ATP. These data suggest that perturbation of the LSGGQ motif might have a greater impact on NBD dimerization than disruption of the Walker A motif. Accordingly, the Walker A lysine mutant K1250A-CFTR is an ATP-dependent channel with moderate P_o (16), whereas the LSGGQ motif mutant G551D-CFTR is an ATP-independent channel with extremely low P_o (14, 33). Thus, the loss of pH_i sensitivity by G551D- and G1349D-CFTR suggests that correct alignment of the NBD1:NBD2 dimer is required for the potentiation of CFTR channel gating by acidic pH_i and inhibition by alkaline pH_i.

Based on several lines of evidence, we suggest that ATP-binding site 2 is a crucial determinant of the pH_i sensitivity of CFTR. First, acidifying pH_i enhances markedly the apparent MgATP affinity of CFTR, whereas alkalinizing pH_i has little effect. Vergani *et al.* (49) argue that K_d values obtained from the [MgATP] dependence of the opening rate of CFTR are a reasonable estimate of the K_d value for ATP binding to site 2. Moreover, using a simple kinetic model of CFTR channel gating, Winter *et al.* (24) demonstrated that the opening rate of CFTR, not its closing rate, is ATP-dependent. These considerations suggest that the pH_i sensitivity of the apparent MgATP affinity of CFTR likely reflect the effects of H^+ ions on the interaction of MgATP with site 2.

Second, our studies of CFTR channel gating in the absence of Mg^{2+} ions demonstrate that Mg^{2+} ions are critical for channel inhibition at alkaline pH_i and modulate channel potentiation at acidic pH_i. Because MgATP binding at both ATP binding sites is a prerequisite for channel opening (50), these data suggest that pH_i has effects on both ATP binding sites. However, Mg^{2+} ions are also a prerequisite for the hydrolysis of ATP that closes the channel (50). This argues that the potentiation of channel gating at pH_i 6.3 is evidence for H^+ ions mediating their effects, at least in part, via site 2.

Third, H^+ ions potentiate the gating behavior of CFTR constructs bearing site-directed mutations in ATP-binding site 1 (K464A- and D572N-CFTR). By contrast, H^+ ions are either without effect (D1370N-CFTR) or inhibit (K1250M-CFTR) the gating behavior of site-directed mutations in ATP-binding site 2. As discussed above, the failure of H^+ ions to potentiate G551D- (site 2) and G1349D-CFTR (site 1) is likely a consequence of the profound disruption of NBD dimerization and, hence, channel gating by these constructs. Taken together, the simplest interpretation of our data is that ATP-binding site 2 is

a crucial determinant of the pH_i sensitivity of the CFTR Cl^- channel (Fig. 9). This suggests that H-bond formation at site 2 enhances channel activity by accelerating NBD dimerization and stabilizing the ATP bound conformation of the NBD1: NBD2 dimer. Consistent with this idea, acidic pH enhanced greatly the formation of an engineered TAP1 homodimer (11).

Mechanism of ATP Hydrolysis at Site 2—A common feature of the ATP binding sites of the ABC transporters CFTR and TAP is their asymmetric ATPase activity (11, 29). In an engineered human TAP1 homodimer, the ATP-binding site with ATPase activity contains a catalytic dyad composed of a histidine residue in the H-loop and a glutamic acid residue distal to the Walker B motif (11, 31). However, instead of hydrolyzing ATP by general base catalysis, this dyad employs substrate-assisted catalysis (SAC) for this reaction (11, 31). In SAC, the interaction of the substrate, ATP, with catalytic water via its γ-phosphate is stabilized by an H-bond between the dyad histidine and the γ-phosphate of ATP (31). A key advantage of SAC over general base catalysis is that it prevents ATP hydrolysis occurring before NBD dimerization (31). In this way so-called "futile ATP hydrolysis" by ABC transporters is avoided.

It is intriguing to consider whether CFTR hydrolyzes ATP at site 2 by SAC. In support of this idea, site 2 but not site 1 contains a catalytic dyad like that found in human TAP1 (11, 29). Although the duration of bursts of channel openings are not determined solely by the ATPase activity of the NBDs (51), the effects of pH_i on the MBD of CFTR (Fig. 3*C*) suggest that alkaline pH_i might enhance ATP hydrolysis at site 2, whereas acidic pH_i has the converse effect. This raises the interesting possibility that the pH_i sensitivity of the ATPase activity at site 2 of CFTR might be similar to the ATP-binding site of an engineered TAP1 homodimer that uses SAC to hydrolyze ATP (11). Finally, in SAC, OH^- ion attack of the γ-phosphate is the rate-limiting step for ATP hydrolysis (11, 31). Taken together, the data suggest that SAC might provide an efficient way to couple NBD dimerization and ATP hydrolysis in the CFTR Cl^- channel. Future studies should explore this possibility.

The pH_i Sensitivity of CFTR Reveals Cross-talk between ATP Binding Sites 1 and 2—An interesting aspect of our data is the pH_i sensitivity of K1250M-CFTR, which is the reverse of that of wild-type CFTR. This observation suggests that there might be hidden minor pH_i effects, masked by the major effects of pH_i on wild-type CFTR. If K1250M-CFTR severely disrupts the function of site 2 (16), these hidden minor pH_i effects might originate from site 1. Our data also reveal that D572N-CFTR has a very unusual response to pH_i: exaggerated potentiation of channel gating at acidic pH_i and potentiation, not inhibition, at alkaline pH_i. In ABC transporters, the Walker B motif is located adjacent to the highly conserved D-loop motif (30, 31). Structural studies of ABC transporters (30, 31) suggest that in CFTR the D-loop of NBD1 (site 1) might (i) interact with the Walker A motif of NBD2 (site 2) and (ii) sense the functional state of site 1 via the H-loop motif of NBD1. In support of this idea, the effects of acidic and alkaline pH_i on D572N-CFTR are reminiscent of the enhanced activity of P574H-CFTR, a CF mutant affecting a residue in the Walker B-D-loop region of NBD1 (52). Thus, the D-loop might mediate cross-talk between the ATP binding sites of CFTR and influence the pH_i sensitivity of CFTR.

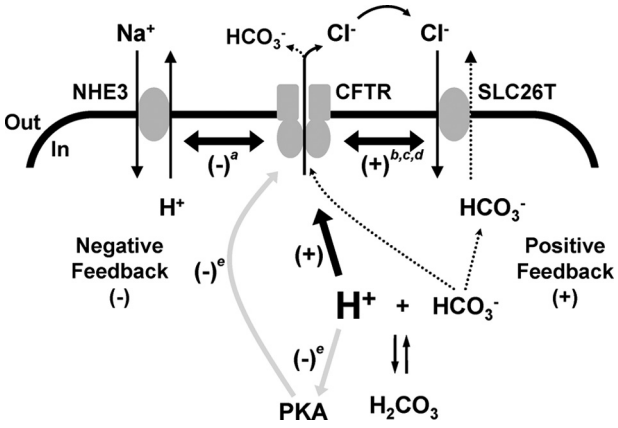

FIGURE 10. **Coordination of the activities of CFTR, NHE3, and SLC26 transporters during acid-base regulation in epithelia.** The simplified models show ion transport by NHE3, CFTR, and SLC26 transporters in the apical membrane of an epithelial cell. *Dotted arrows* indicate the pathways for HCO_3^- secretion from the epithelial cell. The *thick black arrow* denotes the direct regulation of CFTR by protons observed in this study, whereas the *thick double-headed black arrows* represent regulatory interactions between CFTR and either NHE3 or SLC26 transporters (see Refs. 6, 8, 9, and 38). The *gray arrows* indicate the indirect regulation of CFTR by protons through their control of the enzymatic activity of PKA. *SLC26T*, SLC26 transporter; *labels a*, *b*, *c*, *d*, and *e* indicate data from Ahn *et al.* (8), Lee *et al.* (6), Ko *et al.* (38), (9), and Reddy *et al.* (10); (+), stimulation; (−), inhibition. *In* and *Out* denote the intra- and extracellular sides of the membrane, respectively. See "Discussion" for further information.

Identification of pH_i-sensitive Amino Acids in CFTR—The changes in CFTR channel gating at pH_i 6.3 and 8.3 suggest that histidine ($pK_a \sim 6.1$) and cysteine ($pK_a \sim 8.3$) might serve as pH_i-titratable amino acid residues. Examination of the NBD1: NBD2 dimer identifies a number of histidine and cysteine residues located close to the ATP binding sites. Site 1 contains two histidine residues in its LSGGQ motif (His-1348 and His-1350) and a cysteine residue Cys-491 (1, 29). Because Cys-491 is located spatially close to the Walker B aspartate, Asp-572, of site 1 (29), it might modulate the role of Asp-572 in CFTR channel gating by sensing alkaline pH_i. Interestingly, the H-loop of site 2 contains histidine (His-1402) and cysteine (Cys-1400) residues that are lacking in the H-loop of site 1 (29). This raises the interesting possibility that Cys-1400 and His-1402 might act as a pH_i sensor for site 2. However, the potential roles of other histidine and cysteine residues in the control of CFTR channel gating should not be overlooked. For example, the sulfhydryl-modifying reagent *N*-ethylmaleimide rapidly and irreversibly potentiates CFTR channel gating by covalently modifying Cys-832 in the RD (53). Moreover, analyzes of the pH_i dependence of other ion channels (*e.g.* Ref. 35) suggest that other amino acid residues might act as pH_i sensors for CFTR channel gating.

Physiological Significance—Reddy *et al.* (10) demonstrated that pH_i regulates indirectly the CFTR Cl^- conductance of sweat duct epithelia by altering the activity of protein kinases and phosphatases that control RD phosphorylation. By contrast, our data reveal that pH_i regulates directly CFTR channel gating. Taken together, these data suggest that CFTR activity is regulated by pH_i via two different control mechanisms (Fig. 10). First, at the cell membrane localized pH_i fluctuations are

detected directly by CFTR, leading to prompt changes in its behavior, coordinated with alterations in the activity of NHE3 and SLC26 transporters. Second, when there are global changes in pH_i, the effects of pH_i on the enzymes controlling the phosphorylation status of CFTR regulate CFTR indirectly.

Fig. 10 also suggests how the direct and indirect mechanisms of CFTR regulation by pH_i might be integrated in the control of HCO_3^- secretion by epithelial cells. HCO_3^- secretion is driven by the coordinated activity of CFTR and electrogenic SLC26 transporters at the apical membrane (9). Cl^- that exits the cell through CFTR is harnessed by SLC26 transporters to drive HCO_3^- secretion. This efflux of HCO_3^- acidifies pH_i locally in the vicinity of the cell membrane (7), enhancing CFTR channel gating and, hence, Cl^- secretion (Fig. 10). Because CFTR activity is reciprocally coupled to that of SLC26 transporters (9), our data suggest that the two transporters form a positive feedback loop to promote HCO_3^- secretion (Fig. 10). To break this positive feedback loop, a further CFTR control mechanism is required. This is provided by pH_i regulating indirectly RD phosphorylation by controlling enzymatic activity through a negative feedback loop (Fig. 10).

The two-loop model of CFTR regulation by pH_i (Fig. 10) provides a mechanism to control the magnitude and duration of epithelial HCO_3^- secretion. This model might also be exploited to understand better how CF causes aberrant HCO_3^- secretion (37, 38), abnormal pH_i regulation (5, 6), and defects in acidic pH_i-induced apoptosis (54) and bacterial killing (55). Thus, by investigating the effects of pH_i on CFTR, we understand better its mechanism of action, role in fluid and electrolyte transport, and malfunction in CF.

Acknowledgments—We thank L. J. V. Galietta, C. R. O'Riordan, and M. J. Welsh for generous gifts of reagents and L. Schmitt and our departmental colleagues for valuable discussions.

REFERENCES

1. Riordan, J. R., Rommens, J. M., Kerem, B., Alon, N., Rozmahel, R., Grzelczak, Z., Zielenski, J., Lok, S., Plavsic, N., Chou, J. L., Drumm, M. L., Iannuzzi, M. C., Collins, F. S., and Tsui, L. C. (1989) *Science* **245,** 1066–1073
2. Sheppard, D. N., and Welsh, M. J. (1999) *Physiol. Rev.* **79,** S23–S45
3. Gadsby, D. C., Vergani, P., and Csanády, L. (2006) *Nature* **440,** 477–483
4. Welsh, M. J., Ramsey, B. W., Accurso, F., and Cutting, G. R. (2001) in *The Metabolic and Molecular Basis of Inherited Disease* (Scriver, C. R., Beaudet, A. L., Sly, W. S., and Valle, D., eds) pp. 5121–5188, McGraw-Hill Inc., New York
5. Elgavish, A. (1991) *Biochem. Biophys. Res. Commun.* **180,** 342–348
6. Lee, M. G., Wigley, W. C., Zeng, W., Noel, L. E., Marino, C. R., Thomas, P. J., and Muallem, S. (1999) *J. Biol. Chem.* **274,** 3414–3421
7. Poulsen, J. H., Fischer, H., Illek, B., and Machen, T. E. (1994) *Proc. Natl. Acad. Sci. U.S.A.* **91,** 5340–5344
8. Ahn, W., Kim, K. H., Lee, J. A., Kim, J. Y., Choi, J. Y., Moe, O. W., Milgram, S. L., Muallem, S., and Lee, M. G. (2001) *J. Biol. Chem.* **276,** 17236–17243
9. Ko, S. B., Zeng, W., Dorwart, M. R., Luo, X., Kim, K. H., Millen, L., Goto, H., Naruse, S., Soyombo, A., Thomas, P. J., and Muallem, S. (2004) *Nat. Cell Biol.* **6,** 343–350
10. Reddy, M. M., Kopito, R. R., and Quinton, P. M. (1998) *Am. J. Physiol.* **275,** C1040–C1047
11. Ernst, R., Koch, J., Horn, C., Tampé, R., and Schmitt, L. (2006) *J. Biol. Chem.* **281,** 27471–27480
12. Howell, L. D., Borchardt, R., and Cohn, J. A. (2000) *Biochem. Biophys. Res. Commun.* **271,** 518–525
13. Rich, D. P., Berger, H. A., Cheng, S. H., Travis, S. M., Saxena, M., Smith, A. E., and Welsh, M. J. (1993) *J. Biol. Chem.* **268,** 20259–20267
14. Cai, Z., Taddei, A., and Sheppard, D. N. (2006) *J. Biol. Chem.* **281,** 1970–1977
15. Zegarra-Moran, O., Romio, L., Folli, C., Caci, E., Becq, F., Vierfond, J. M., Mettey, Y., Cabrini, G., Fanen, P., and Galietta, L. J. (2002) *Br. J. Pharmacol.* **137,** 504–512
16. Carson, M. R., Travis, S. M., and Welsh, M. J. (1995) *J. Biol. Chem.* **270,** 1711–1717
17. Elroy-Stein, O., Fuerst, T. R., and Moss, B. (1989) *Proc. Natl. Acad. Sci. U.S.A.* **86,** 6126–6130
18. Rich, D. P., Anderson, M. P., Gregory, R. J., Cheng, S. H., Paul, S., Jefferson, D. M., McCann, J. D., Klinger, K. W., Smith, A. E., and Welsh, M. J. (1990) *Nature* **347,** 358–363
19. Anderson, M. P., Rich, D. P., Gregory, R. J., Smith, A. E., and Welsh, M. J. (1991) *Science* **251,** 679–682
20. Sheppard, D. N., and Robinson, K. A. (1997) *J. Physiol.* **503,** 333–346
21. Vergani, P., Nairn, A. C., and Gadsby, D. C. (2003) *J. Gen. Physiol.* **121,** 17–36
22. Ikuma, M., and Welsh, M. J. (2000) *Proc. Natl. Acad. Sci. U.S.A.* **97,** 8675–8680
23. Lansdell, K. A., Cai, Z., Kidd, J. F., and Sheppard, D. N. (2000) *J. Physiol.* **524,** 317–330
24. Winter, M. C., Sheppard, D. N., Carson, M. R., and Welsh, M. J. (1994) *Biophys. J.* **66,** 1398–1403
25. Li, H., and Sheppard, D. N. (2009) *BioDrugs* **23,** 203–216
26. Woodhull, A. M. (1973) *J. Gen. Physiol.* **61,** 687–708
27. Tabcharani, J. A., Rommens, J. M., Hou, Y. X., Chang, X. B., Tsui, L. C., Riordan, J. R., and Hanrahan, J. W. (1993) *Nature* **366,** 79–82
28. Vergani, P., Lockless, S. W., Nairn, A. C., and Gadsby, D. C. (2005) *Nature* **433,** 876–880
29. Lewis, H. A., Buchanan, S. G., Burley, S. K., Conners, K., Dickey, M., Dorwart, M., Fowler, R., Gao, X., Guggino, W. B., Hendrickson, W. A., Hunt, J. F., Kearins, M. C., Lorimer, D., Maloney, P. C., Post, K. W., Rajashankar, K. R., Rutter, M. E., Sauder, J. M., Shriver, S., Thibodeau, P. H., Thomas, P. J., Zhang, M., Zhao, X., and Emtage, S. (2004) *EMBO J.* **23,** 282–293
30. Smith, P. C., Karpowich, N., Millen, L., Moody, J. E., Rosen, J., Thomas, P. J., and Hunt, J. F. (2002) *Mol. Cell* **10,** 139–149
31. Hanekop, N., Zaitseva, J., Jenewein, S., Holland, I. B., and Schmitt, L. (2006) *FEBS Lett.* **580,** 1036–1041
32. Hopfner, K. P., Karcher, A., Shin, D. S., Craig, L., Arthur, L. M., Carney, J. P., and Tainer, J. A. (2000) *Cell* **101,** 789–800
33. Bompadre, S. G., Sohma, Y., Li, M., and Hwang, T. C. (2007) *J. Gen. Physiol.* **129,** 285–298
34. Zifarelli, G., Murgia, A. R., Soliani, P., and Pusch, M. (2008) *J. Gen. Physiol.* **132,** 185–198
35. Schulte, U., Hahn, H., Konrad, M., Jeck, N., Derst, C., Wild, K., Weidemann, S., Ruppersberg, J. P., Fakler, B., and Ludwig, J. (1999) *Proc. Natl. Acad. Sci. U.S.A.* **96,** 15298–15303
36. Roos, A., and Boron, W. F. (1981) *Physiol. Rev.* **61,** 296–434
37. Choi, J. Y., Muallem, D., Kiselyov, K., Lee, M. G., Thomas, P. J., and Muallem, S. (2001) *Nature* **410,** 94–97
38. Ko, S. B., Shcheynikov, N., Choi, J. Y., Luo, X., Ishibashi, K., Thomas, P. J., Kim, J. Y., Kim, K. H., Lee, M. G., Naruse, S., and Muallem, S. (2002) *EMBO J.* **21,** 5662–5672
39. McCarty, N. A., McDonough, S., Cohen, B. N., Riordan, J. R., Davidson, N., and Lester, H. A. (1993) *J. Gen. Physiol.* **102,** 1–23
40. Linsdell, P. (2005) *J. Biol. Chem.* **280,** 8945–8950
41. Cai, Z., Lansdell, K. A., and Sheppard, D. N. (1999) *Br. J. Pharmacol.* **128,** 108–118
42. Zhou, Z., Hu, S., and Hwang, T. C. (2002) *J. Gen. Physiol.* **120,** 647–662
43. Zhang, Z. R., Zeltwanger, S., and McCarty, N. A. (2004) *J. Membr. Biol.* **199,** 15–28
44. Sigel, H., and Griesser, R. (2005) *Chem. Soc. Rev.* **34,** 875–900
45. Ostedgaard, L. S., Baldursson, O., Vermeer, D. W., Welsh, M. J., and Rob-

ertson, A. D. (2000) *Proc. Natl. Acad. Sci. U.S.A.* **97,** 5657–5662
46. Baker, J. M., Hudson, R. P., Kanelis, V., Choy, W. Y., Thibodeau, P. H., Thomas, P. J., and Forman-Kay, J. D. (2007) *Nat. Struct. Mol. Biol.* **14,** 738–745
47. Wilkinson, D. J., Strong, T. V., Mansoura, M. K., Wood, D. L., Smith, S. S., Collins, F. S., and Dawson, D. C. (1997) *Am. J. Physiol.* **273,** L127–L133
48. Scott-Ward, T. S., Cai, Z., Dawson, E. S., Doherty, A., Da Paula, A. C., Davidson, H., Porteous, D. J., Wainwright, B. J., Amaral, M. D., Sheppard, D. N., and Boyd, A. C. (2007) *Proc. Natl. Acad. Sci. U.S.A.* **104,** 16365–16370
49. Vergani, P., Basso, C., Mense, M., Nairn, A. C., and Gadsby, D. C. (2005) *Biochem. Soc. Trans.* **33,** 1003–1007
50. Dousmanis, A. G., Nairn, A. C., and Gadsby, D. C. (2002) *J. Gen. Physiol.* **119,** 545–559
51. Ramjeesingh, M., Li, C., Garami, E., Huan, L. J., Galley, K., Wang, Y., and Bear, C. E. (1999) *Biochemistry.* **38,** 1463–1468
52. Sheppard, D. N., Ostedgaard, L. S., Winter, M. C., and Welsh, M. J. (1995) *EMBO J.* **14,** 876–883
53. Cotten, J. F., and Welsh, M. J. (1997) *J. Biol. Chem.* **272,** 25617–25622
54. Barrière, H., Poujeol, C., Tauc, M., Blasi, J. M., Counillon, L., and Poujeol, P. (2001) *Am. J. Physiol.* **281,** C810–C824
55. Di, A., Brown, M. E., Deriy, L. V., Li, C., Szeto, F. L., Chen, Y., Huang, P., Tong, J., Naren, A. P., Bindokas, V., Palfrey, H. C., and Nelson, D. J. (2006) *Nat. Cell Biol.* **8,** 933–944